IEEE Access
Multidisciplinary | Rapid Review | Open Access Journal

Received March 27, 2019, accepted April 13, 2019, date of publication April 22, 2019, date of current version May 2, 2019.

Digital Object Identifier 10.1109/ACCESS.2019.2912216

Hybrid Multi-Carrier PWM Technique Based on Carrier Reconstruction for Cascaded H-bridge Inverter

MANYUAN YE, LE CHEN, LIXUAN KANG, SONG LI, JUNFEI ZHANG, AND HAN WU
College of Electrical and Automation Engineering, East China Jiaotong University, Nanchang 330013, China

Corresponding author: Manyuan Ye (yemanyuan1@163.com)

This work was supported in part by the National Natural Science Foundation of China and Award Number under Grant 51767007, and in part by the Natural Science Foundation of Jiangxi Provincial Department of Education under Grant GJJ180306.

ABSTRACT In response to the deficiencies that the Carrier Phase Shift (CPS-PWM) and Carrier In-Phase Disposition (IPD-PWM) modulation techniques are applied to Cascaded H-bridge (CHB) multilevel inverters, combined with the advantages of the two techniques, a Hybrid Multi-carrier PWM technique based on carrier reconstruction is proposed. The aforementioned technique uses the carrier segment in the half carrier period of the IPD-PWM technique as the basic unit and optimizes the modulation performance by periodically adjusting its arrangement in the vertical direction. When CHB multilevel inverter adopts Hybrid Multi-carrier PWM technique, as with CPS-PWM technique, the output power balance between the cascaded H-bridge cells is achieved naturally; at the same time, the harmonic spectrum of the output voltage is identical with that of the IPD-PWM technique, that is to say, the harmonic characteristics of the output line voltage of the inverters are effectively improved. In this paper, the CHB seven-level inverter is taken as an example, and the correctness of the relevant conclusions is verified by simulation and experimental results.

INDEX TERMS Hybrid multi-carrier PWM, cascaded H-bridge inverter, power balance, harmonics analysis.

I. INTRODUCTION

In recent years, multilevel inverters have the advantages of less power semiconductor device stress, good harmonic characteristics of the output voltage, and low switching loss, etc. In the fields of medium and high voltage speed regulation, High-voltage direct current transmission and AC flexible direct current transmission systems, etc. It has been widely used [1]–[3]. As the most common multilevel converter, the CHB multilevel inverter has become a widely used topology because of its nearly ideal sinusoidal waveforms, simple controlling and easy assembling [4], [5].

The modulation technique of multilevel inverters is the key link for outputting superior multilevel waveforms, which directly determines the waveform quality of the output voltage and the output power distribution between cascaded H-bridge cells. At present, the common modulation techniques applied to CHB inverters can be classified into low frequency modulation techniques and high frequency modulation techniques according to the device switching frequency. Low-frequency modulation techniques mainly include staircase wave synthesis [6] and Selective Harmonic Elimination (SHE) [7]. Although the low-frequency modulation technique has lower switching losses, the quality of output waveforms and dynamic response performance are poor. High-frequency modulation techniques mainly include CPS-PWM [8], IPD-PWM [9] and Space Vector Modulation (SVM) [10] techniques. Among them, CPS-PWM technique can achieve output power balance naturally between cascaded H-bridge cells, but the THD of line voltage u_{AB} is higher with this technique, especially at low amplitude modulation index [11], [12]; IPD-PWM technique can minimize harmonic content of line voltage u_{AB}, but can't naturally balance the output power between cascaded H-bridge cells [13]–[15]. The imbalanced output power between cascaded H-bridge cells will cause the discharging characteristics of DC source to be inconsistent, resulting in deviation of DC source voltage, at the same time, the service life of DC source will be greatly different, and the maintenance cost will be increased.

The associate editor coordinating the review of this manuscript and approving it for publication was Nataraj Prabaharan.

In order to solve the problem of imbalanced output power between cascaded H-bridge cells under IPD-PWM modulation technique, it is necessary to optimize and improve IPD-PWM technique. The literature [16], [17] proposes a hybrid multi-carrier PWM technique, which can achieve output power balance naturally between cascaded H-bridge cells and has lower harmonic content of line voltage u_{AB} than CPS-PWM technique at low amplitude modulation index when this modulation technique is applied to CHB Seven-level inverters, but at high modulation index, the THD of u_{AB} is the same as the CPS-PWM technique. When this modulation technique is applied to the five-level CHB inverter, the THD of u_{AB} is the same as the CPS-PWM technique in the full modulation index range. The literature [18] improves the output power imbalance between cascaded H-bridge cells by cyclically moving modulation waves in different carrier regions, but this method is only for applications where the modulation index is less than 0.5. The literature [19] proposes a power balance control method based on one output period. By adjusting the carrier amplitude in one output period, the output power of each cascaded H-bridge cell is changed, and the output power imbalance caused by space is compensated in time. However, it takes a long time for power balance when the number of cascaded H-bridge cell is large.

In view of the shortcomings of various improved modulation techniques proposed in the above literature. Therefore, it is of great significance to study a modulation technique which can not only make the output line voltage of the inverters have the best harmonic characteristics, but also realize the output power balance between cascaded cells. and the time required for power balance is short in the full modulation index range.

In this paper, the CHB Seven-level inverter is taken as the research object, Firstly, the working principle of CPS-PWM and IPD-PWM modulation techniques and output voltage characteristics under the two techniques are briefly analyzed, and the shortcomings of their application in CHB multilevel inverters are pointed out. Then, by reconstructing the triangular carrier in IPD-PWM technique, a Hybrid Multi-carrier PWM modulation technique is proposed, which combines the advantages of CPS-PWM and IPD-PWM techniques. It can not only make the harmonic characteristics of output line voltage exactly the same as IPD-PWM technique, but also retain the advantage of CPS-PWM technique that can naturally balance the output power between cascaded H-bridge cells. Finally, Simulation and experimental results are provided to demonstrate the validity of the proposed method.

II. CHB INVERTER AND ITS MODULATION TECHNIQUE

A. TOPOLOGY AND ITS WORKING PRINCIPLE

The CHB seven-level inverter topology is shown in Fig. 1. u_{H1}, u_{H2}, and u_{H3} are the output voltage of three cascaded H-bridge cells respectively, u_{AN} is the output phase voltage of inverter, and i_o is the output current. According to the basic working principle of CHB inverters, each H-bridge cell can

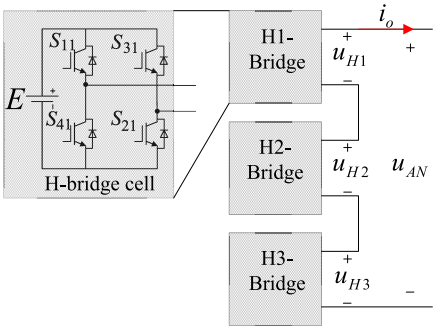

FIGURE 1. Topology of CHB seven-level inverter.

output three levels (-E, 0, E), and the output phase voltage u_{AN} has seven levels: $\pm 3E$, $\pm 2E$, $\pm E$, 0.

Suppose s_i be a switching function of cascaded cell i (i = 1, 2, 3) output level state. When $u_{Hi} = E$, then $s_i = 1$; when $u_{Hi} = 0$, then $s_i = 0$; and when $u_{Hi} =$ -E, then $s_i = -1$. Then the output voltage u_{Hi} of cascade cell i can be expressed as

$$u_{Hi} = s_i E \tag{1}$$

Further, the output phase voltage u_{AN} of the inverter can be expressed as

$$u_{AN} = E \sum_{i=1}^{3} s_i \tag{2}$$

In order to avoid the mutual transfer of power between cascaded cells, the output voltage of cascaded cells remains unipolar, that is, when u_{AN} is positive, u_{Hi} can only be E or 0; when u_{AN} is negative, u_{Hi} can only be -E or 0.

The switching function of the inverter output level state is defined as S, and $S = (S_1 S_2 S_3)$. According to the formula (2), Table 1 gives the output level of the inverter under different switching functions. It is obvious from the table that when the output level of the inverter is $\pm 3E$ and $\pm 2E$, there are redundant switching function states.

B. TWO COMMON MUILTI-CARRIER PWM TECHNIQUES

For the CHB seven-level inverter, IPD-PWM technique requires six triangular carriers with the same amplitude, frequency, and phase. Fig.2 shows the modulation principle of IPD-PWM technique, where v_m is the sinusoidal modulation wave, v_{cri} and v_{cri-} are a pair of triangular carrier signals for each H-bridge cell i. Under IPD-PWM technique, the output voltage u_{H1}, u_{H2} and u_{H3} of the three H-bridge cells has obvious difference in pulse width. Especially at low modulation index relatively, the output voltage of some cascaded cells is always equal to 0, at this time, there is a serious problem of imbalanced output power among the cascaded cells.

The CPS-PWM modulation technique makes full use of the redundant switching function state of the output level of the inverters to realize the output power balance naturally between the cascaded cells. The modulation principle is shown in Fig.3. For the CHB seven-level inverter,

TABLE 1. Relationship between the output level and switching function of the inverter.

u_{AN}	Switch Function		
	S_1	S_2	S_3
$3E$	1	1	1
$2E$	1	1	0
	1	0	1
	0	1	1
E	1	0	0
	0	1	0
	0	0	1
0	0	0	0
$-E$	-1	0	0
	0	-1	0
	0	0	-1
$-2E$	-1	-1	0
	0	-1	-1
	-1	0	-1
$-3E$	-1	-1	-1

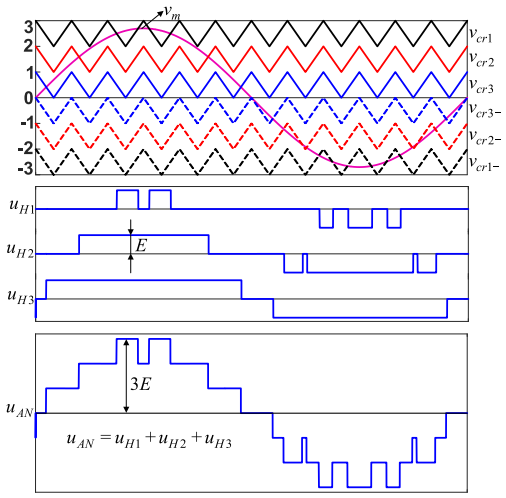

FIGURE 2. Principle of IPD-PWM.

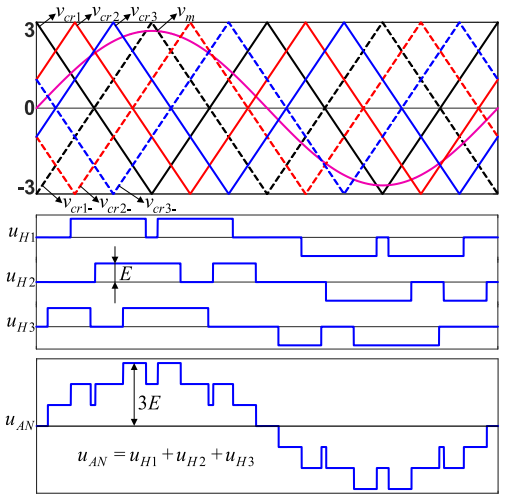

FIGURE 3. Principle of CPS-PWM.

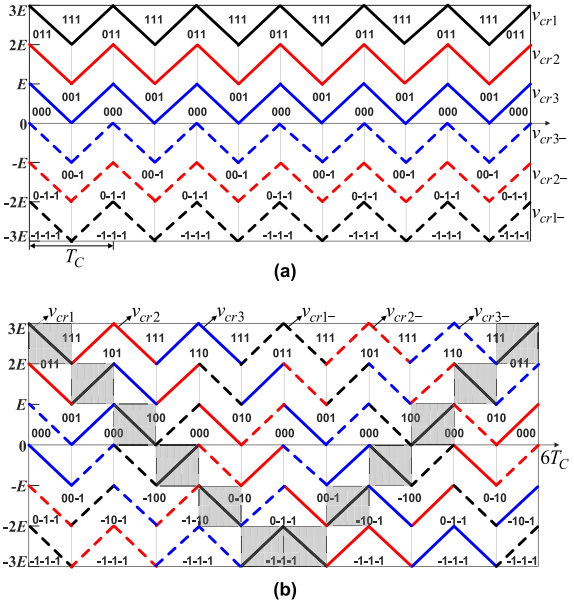

FIGURE 4. Carrier reconstruction diagram. (a) Before carrier reconstruction. (b) After carrier reconstruction.

CPS-PWM technique requires six triangular carriers with the same amplitude and frequency, and the phase shift among the carriers is 60°. Each bridge arm corresponds to a triangular carrier, and each cascaded H-bridge cell corresponds to a pair of inverted triangular carrier wave, v_{cri} and v_{cri-}. The waveforms of u_{Hi} are the same, just the difference in phases, and the output power balance between the cascaded H-bridge cells can be realized naturally.

III. HYBRID MULTI-CARRIER PWM TECHNIQUE

In order to combine the advantages of CPS-PWM and IPD-PWM techniques, this paper reconstructs the triangular carrier of IPD-PWM technique for CHB Seven-level inverters, and proposes a new power balance modulation technique. On one hand, the proposed modulation technique retains the advantage that CPS-PWM technique can naturally balance the output power between cascaded H-bridge cells; on the other hand, it adds the advantage of IPD-PWM technique that the output line voltage of inverters has the best harmonic characteristics.

A. CARRIER RECONSTRUCTION PRINCIPLE AND HARMONIC ANALYSIS

The carrier reconstruction principle of Hybrid Multi-carrier PWM technique is shown in Fig.4. In the carriers of IPD-PWM technique, the triangular carrier period is set as T_C, and the carrier segment in the half carrier period $\frac{T_C}{2}$ is taken as the basic unit. At the end of each half carrier period, the

carrier segment is moved vertically once, and after 12 times of movement, a cycle is completed. At this time, the period of reconstructed carrier is $6T_C$. As shown in Fig. 4(b), the carrier segments in the 12 shaded regions constitute one reconstructed carrier in the Hybrid Multi-carrier PWM technique, the remaining five reconstructed carriers is obtained by sequentially shifting one sixth of the reconstructed carrier period in phase. Thus, all the reconstructed carriers of Hybrid Multi-carrier PWM technique applied to CHB Seven-level inverters are obtained. Each cascaded cell corresponds to a pair of reconstructed carrier signals v_{cri} and v_{cri-} in Fig. 4(b).

According to the logical relationship between the modulation wave and carrier waves, the switching function S of inverter output level state can be obtained when the modulation wave is in different regions. Fig.4 shows the comparison of switching function S before and after carrier reconstruction. In Fig. 4(a), IPD-PWM technique has only seven switching function states: 111, 011, 001, 000, 00−1, 0−1 − 1 and −1 − 1 − 1, which correspond to the output phase voltages of the inverters $3E$, $2E$, E, 0, $-E$, $-2E$, and $-3E$, respectively. The switching function S after carrier reconstruction is shown in Fig. 4(b). By comparison, it is found that when the output voltage u_{AN} is $2E$, E, $-E$, $-2E$, Hybrid Multi-carrier PWM technique makes use of the eight redundant switching function states of 101, 110, 100, 010, −100, 0−10, −10 − 1 and −1 − 10, but does not change the output voltage u_{AN} of the inverters. Therefore, the inverter output voltage waveform obtained by respectively comparing the same modulation wave with the two carriers of Fig. 4(a) and (b) is completely the same, and the harmonic spectrum is completely identical.

Suppose ω_s is the fundamental wave angle frequency, m_a is the amplitude modulation index, the triangular carrier frequency of IPD-PWM technique is f_c, and the angular frequency is ω_c, thus the sinusoidal modulation wave can be expressed as

$$v_m = 3m_a \sin(w_s t) \tag{3}$$

Using the double Fourier series analysis method, the harmonic expression of the output phase voltage u_{AN} under IPD-PWM technique can be given by [13]

$$\begin{aligned} &u_{IPD\_AN}(t) \\ &\quad = 3m_a E \sin(w_s t) \\ &\qquad + \sum_{m=1}^{\infty}\sum_{n=-\infty}^{\infty} \{B_P(m,n) \sin[(2m\text{-}1)w_c t + 2nw_s t]\} \\ &\qquad + \sum_{m=1}^{\infty}\sum_{n=-\infty}^{\infty} \{C_P(m,n) \sin[2mw_c t + (2n\text{-}1)w_s t]\} \end{aligned} \tag{4}$$

According to the previous analysis, the output phase voltage waveform of the inverter under the Hybrid Multi-carrier PWM technique proposed in this paper is exactly the same as that under the IPD-PWM technique. and the reconstructed carrier is 6 times the period of the triangular carrier of IPD-PWM technique. Suppose the reconstructed carrier period is $T_C^{'}$, the frequency is $f_c^{'}$, and the angular frequency is $\omega_c^{'}$. Then the relationship expression between the angular frequency before and after carrier reconstruction always satisfies the following equation:

$$\omega_c = 6\omega_c' \tag{5}$$

Substituting equation (5) into equation (4), it can be concluded that under Hybrid Multi-carrier PWM technique, the harmonic expression of the u_{AN} is

$$\begin{aligned} &u_{Hybrid\_Multi-carrier_{AN}}(t) \\ &\quad = 3m_a E \sin(w_s t) \\ &\qquad + \sum_{m=1}^{\infty}\sum_{n=-\infty}^{\infty} \left\{B_P(m,n) \sin\left[(2m\text{-}1)\cdot 6w_c' t + 2nw_s t\right]\right\} \\ &\qquad + \sum_{m=1}^{\infty}\sum_{n=-\infty}^{\infty} \left\{C_P(m,n) \sin\left[2m\cdot 6w_c' t + (2n\text{-}1)w_s t\right]\right\} \end{aligned} \tag{6}$$

In the formulas (4) and (6), $B_P(m,n)$ and $C_P(m,n)$ are harmonic amplitudes of u_{AN}, and their mathematical expressions are respectively

$$\begin{aligned} B_P(m,n) = &\frac{8E}{\pi^2(2m-1)} \cdot \\ &\sum_{k=0}^{\infty}\left\{\frac{J_{2k+1}[2\pi(2m-1)m_a]\cdot(-1)^k}{(2k+1)^2-4n^2}\right. \\ &\left.\cdot(2k+1)\cos(n\pi)\right\} \end{aligned} \tag{7}$$

$$C_P(m,\mathrm{n}) = \frac{E}{\pi m}\cdot J_{2n-1}(4m\pi m_a) \tag{8}$$

In the formula, $J_{2n-1}(4m\pi m_a)$ is the Bessel function.

It can be seen from the equations (4) and (6) that the fundamental component of u_{AN} is E times over the modulation wave v_m, and its amplitude is proportional to the modulation index m_a. When $m = 1$, under IPD-PWM technique, the lowest harmonics of u_{AN} are mainly the even-numbered sideband harmonics centered around f_c; under Hybrid Multi-carrier PWM technique, the lowest harmonic of u_{AN} are mainly the even-numbered sideband harmonics centered around $6f_c'$. Since equation (5) is always true, under the two modulation techniques, the spectrum distribution of u_{AN} is exactly the same.

B. POWER BALANCE ANALYSIS

Fig.5 shows the modulation principle of Hybrid Multi-carrier PWM technique. Compared with the modulation principle of IPD-PWM technique shown in Fig. 2, it can be seen that the proposed technique utilizes the redundant switching function states of the inverter, the output voltage characteristics of each cascaded H-bridge cell can be changed by adjusting the arrangement of carriers in vertical direction, but the output level state of the inverters can not be changed. This creates conditions for realizing power balance control between cascaded cells.

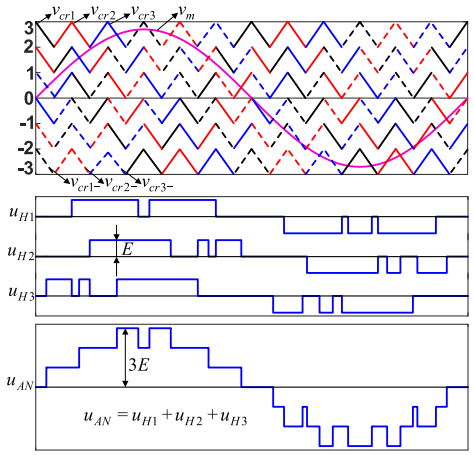

FIGURE 5. Principle of Hybrid Multi-carrier PWM.

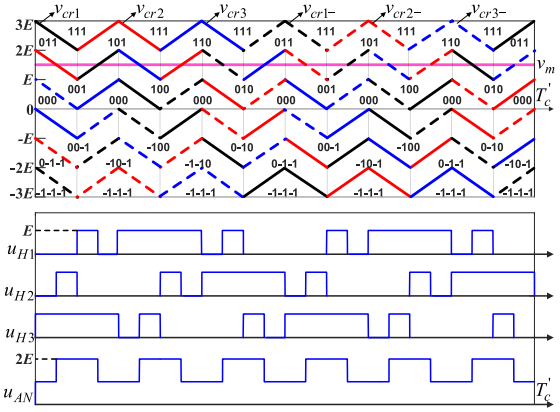

FIGURE 6. Analysis of power balance control over the output positive half cycle.

In order to explain the principle of power balance with Hybrid Multi-carrier PWM technique, the output voltage characteristics of the cascaded cells are analyzed over the reconstructed carrier period. It is assumed that the reconstructed carrier frequency $f_c^{'}$ is much larger than the sinusoidal modulation wave frequency f_s, then the modulation wave v_m and the inverter output current i_o can be regarded as constant values over a reconstructed carrier period.

Fig. 6 shows the output voltage of cascaded cells and inverters under Hybrid Multi-carrier PWM technique over the output positive half cycle. The figure is illustrated by the example of the output voltage of the inverter which located in the interval $[E, 2E]$. t_{Hi+} indicates the time when u_{Hi} is equal to E during the reconstructed carrier period, then t_{Hi+} can be expressed as

$$\begin{cases} t_{H1+} = \dfrac{T_C^{'}}{3} v_m \\ t_{H2+} = \dfrac{T_C^{'}}{3} v_m \\ t_{H3+} = \dfrac{T_C^{'}}{3} v_m \end{cases} \tag{9}$$

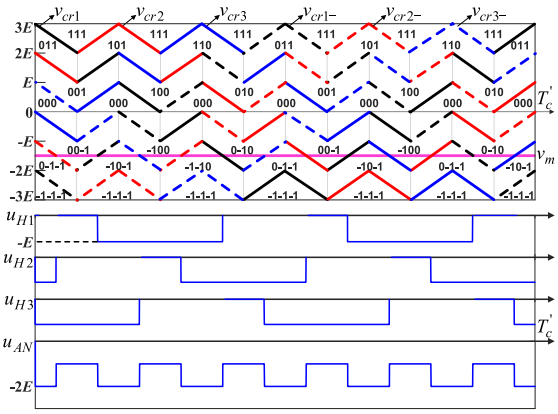

FIGURE 7. Analysis of power balance control over the output negative half cycle.

The output voltage average values $\bar{u}_{H1+}$, $\bar{u}_{H2+}$, and $\bar{u}_{H3+}$ of the cascaded H-bridge cells over the reconstructed carrier cycle are respectively

$$\begin{cases} \bar{u}_{H1+} = \dfrac{v_m}{3} E \\ \bar{u}_{H2+} = \dfrac{v_m}{3} E \\ \bar{u}_{H3+} = \dfrac{v_m}{3} E \end{cases} \tag{10}$$

Since the output current of each cascaded H-bridge cell are equal and constant, it can be known from the equation (10) that over the reconstructed carrier period, the output power average values of each cascaded cell $\bar{P}_{H1+}$, $\bar{P}_{H2+}$, and $\bar{P}_{H3+}$ is equal, which is

$$\bar{P}_{H1+} = \bar{P}_{H2+} = \bar{P}_{H3+} \tag{11}$$

Fig. 7 shows the output voltage of cascaded cells and inverters under Hybrid Multi-carrier PWM technique over the output negative half cycle. The figure is illustrated by the example of the output voltage of the inverter which located in the interval $[-2E, -E]$. t_{Hi-} indicates the time when u_{Hi} is equal to -E during the reconstructed carrier period, then t_{Hi-} can be expressed as

$$\begin{cases} t_{H1-} = \dfrac{T_C^{'}}{3} v_m \\ t_{H2-} = \dfrac{T_C^{'}}{3} v_m \\ t_{H3-} = \dfrac{T_C^{'}}{3} v_m \end{cases} \tag{12}$$

The output voltage average values $\bar{u}_{H1-}$, $\bar{u}_{H2-}$, and $\bar{u}_{H3-}$ of the cascaded H-bridge cells over the reconstructed carrier

TABLE 2. Simulation parameters.

parameters	Numerical value
DC voltage E/V	100
Amplitude modulation index m_a	0.9
Reconstructed carrier frequency $f_c^{'}$/HZ	550
Fundamental frequency f_s/HZ	50
Filter inductor L/mH	4
Load Resistance R/ Ω	20

cycle are respectively

$$\begin{cases} \bar{u}_{H1-} = \dfrac{v_m}{3}E \\ \bar{u}_{H2-} = \dfrac{v_m}{3}E \\ \bar{u}_{H3-} = \dfrac{v_m}{3}E \end{cases} \tag{13}$$

It can be known from the equation (13) that over the reconstructed carrier period, the output power average values of each cascaded cell $\bar{P}_{H1-}$, $\bar{P}_{H2-}$, and $\bar{P}_{H3-}$ is equal, which is

$$\bar{P}_{H1-} = \bar{P}_{H2-} = \bar{P}_{H3-} \tag{14}$$

Therefore, on the basis of IPD-PWM technique, the carrier is reconstructed by changing the arrangement of carriers in the vertical direction, so that the output voltage average values of each cascaded cell is equal over the reconstructed carrier cycle, thus ensuring that the output power average values of each cascaded cell is equal and the time required for power balance is one reconstructed carrier period.

IV. SIMULATION ANALYSIS

In order to verify the correctness of Hybrid Multi-carrier PWM technique proposed in this paper, the topology AC side shown in Fig.1 is connected to the filter inductor and the load resistor, it is simulated and analyzed with MATLAB/Simulink software. The simulation parameters are shown in Table 2.

Fig.8 shows the simulated voltage and current waveforms with Hybrid Multi-carrier PWM technique. The waveforms of u_{H1}, u_{H2}, and u_{H3} are almost identical except for a small phase displacement caused by the phase-shifted carriers. The phase voltage u_{AN} is a seven-level PWM waveform, and the current i_o is a sine wave with a better waveform quality.

Fig.9 shows the harmonic spectrum of the inverter output current i_o under Hybrid Multi-carrier PWM technique. It can be seen from the figure that the high-frequency harmonic components mainly concentrate on the $6f_c^{'}$ and its side-band harmonics, such as $6f_c^{'}$ and $6f_c^{'} \pm 2f_s$ in the figure, in which $6f_c^{'}$ is the main low-order carrier harmonic. The THD value of i_o is only 4.47%. If the reconstructed carrier frequency $f_c^{'}$ is increased, the THD value will be lower and the harmonic performance will be better.

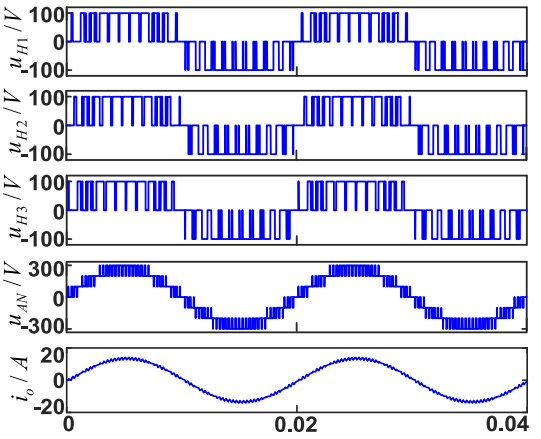

FIGURE 8. Simulation waveform.

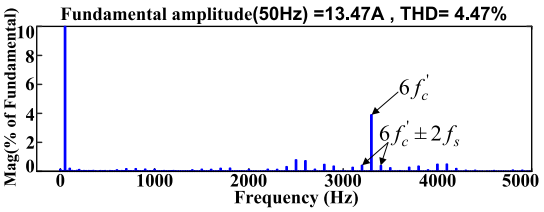

FIGURE 9. Harmonic Spectrum of i_o.

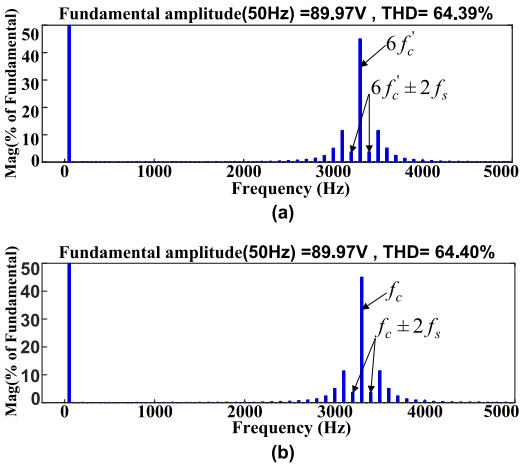

FIGURE 10. Harmonic Spectrum of u_{AN}(m_a = 0.3). (a) with Hybrid Multi-carrier PWM technique. (b) with IPD-PWM technique.

Fig.10 shows the harmonic spectrum of u_{AN} with Hybrid Multi-carrier PWM and IPD-PWM techniques respectively at $m_a = 0.3$.

Fig.11 shows the harmonic spectrum of u_{AN} with Hybrid Multi-carrier PWM and IPD-PWM techniques respectively at $m_a = 0.6$.

Fig.12 shows the harmonic spectrum of u_{AN} with Hybrid Multi-carrier PWM and IPD-PWM techniques respectively at $m_a = 0.9$.

Since equation (5) is always true, the carrier frequency f_c of IPD-PWM technique should be set to 3300 Hz. It can be seen from the comparison that the spectrum distribution of

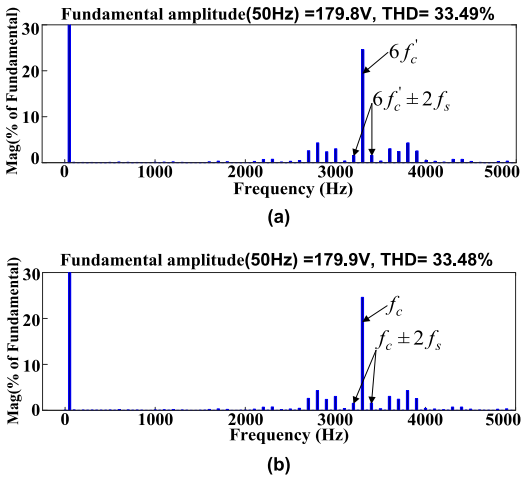

FIGURE 11. Harmonic Spectrum of $u_{AN}(m_a = 0.6)$. (a) with Hybrid Multi-carrier PWM technique. (b) with IPD-PWM technique.

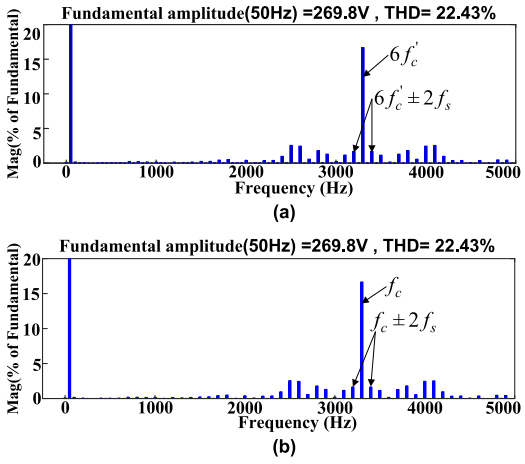

FIGURE 12. Harmonic Spectrum of $u_{AN}(m_a = 0.9)$. (a) with Hybrid Multi-carrier PWM technique. (b) with IPD-PWM technique.

u_{AN} is exactly the same under the two modulation techniques. With Hybrid Multi-carrier PWM technique, the harmonics of the phase voltage u_{AN} are mainly even-numbered sideband harmonics centered on $6f_c'$, such as $6f_c'$ and $6f_c' \pm 2f_s$ in the figure, in which $6f_c'$ is the main low-order carrier harmonic, the fundamental amplitude of u_{AN} is also equal to $300m_a$. The harmonic distribution and fundamental amplitude of u_{AN} under IPD-PWM technique are the same as those of Hybrid Multi-carrier technique. These simulation results are consistent with the previous harmonic theory analysis.

Because the harmonic spectrum of the phase voltage u_{AN} is identical, the harmonic spectrum of the line voltage u_{AB} is identical. Therefore, Hybrid Multi-carrier PWM technique retains the advantage of IPD-PWM technique that the output line voltage of inverters has the optimal harmonic characteristics

The variations in the THD of u_{AB} with m_a is shown in Fig.13 when the CHB seven-level inverter adopts the three techniques. It can be seen from the figure that under the Hybrid Multi-carrier PWM and IPD-PWM technique,

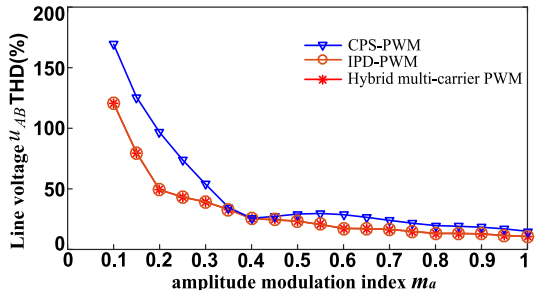

FIGURE 13. Variations of line voltage THDs with m_a.

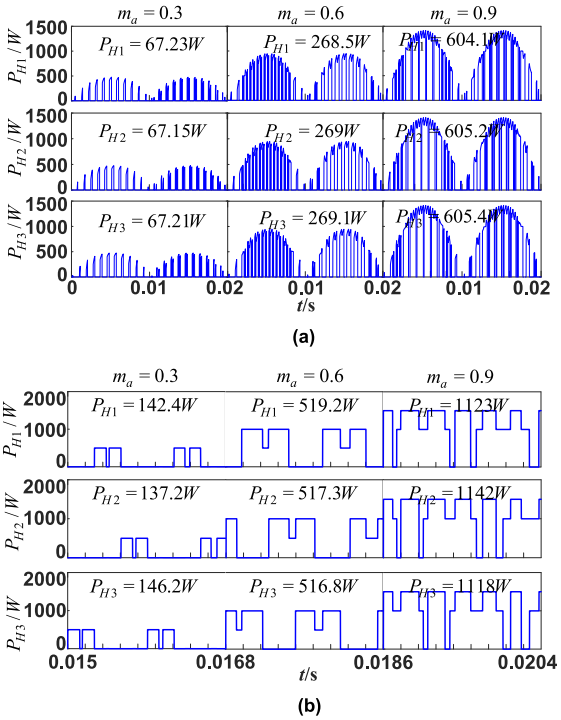

FIGURE 14. Output power of each cell at different m_a. (a) Output power over the output cycle. (b) Output power over the reconstructed carrier cycle.

the THD value of u_{AB} is equal and is the lowest in the full modulation index range.

Fig.14(a) shows the simulation waveforms of the instantaneous output power $p_{Hi}(i = 1, 2, 3)$ of H1, H2 and H3 cells at three amplitude modulation indexs. It can be seen from the figure that the average output power of each cascaded H-bridge cell is equal at different modulation indexs, and the power balance control is realized. Fig. 14(b) shows the simulation waveforms of the instantaneous output power p_{Hi} of each cascaded cell over the reconstructed carrier cycle at three amplitude modulation indexs. As can be seen from the figure, the ratio of the average output power between the cascaded cells is approximately equal to 1:1:1. Therefore, Hybrid Multi-carrier PWM technique proposed in this paper can achieve power balance between cascaded cells in one reconstructed carrier period T_C'.

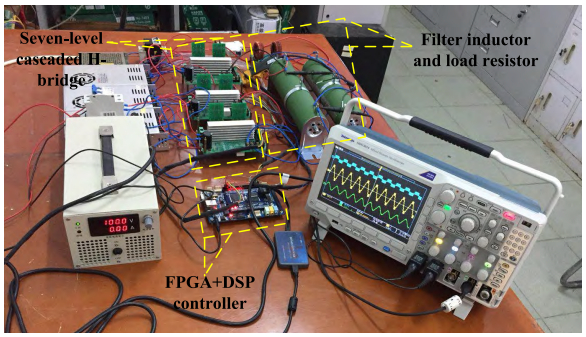

FIGURE 15. Experimental prototype.

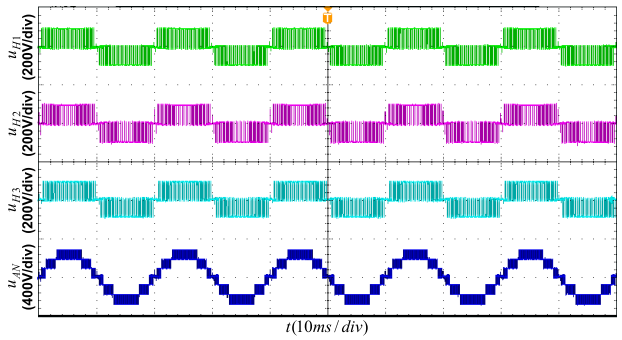

FIGURE 16. Output voltages of cascaded cells and the inverter.

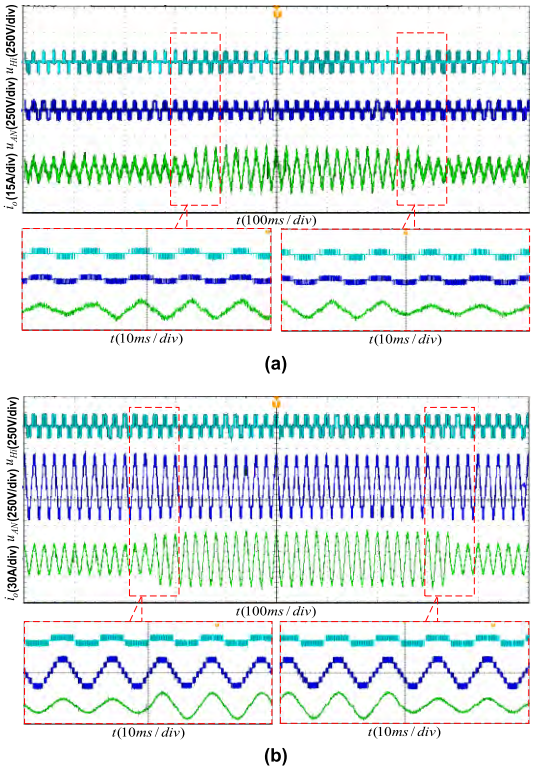

FIGURE 17. Dynamic experiment waveforms. (a) $m_a = 0.3$. (b) $m_a = 0.9$.

V. EXPERIMENT

In order to further verify the feasibility of the proposed Hybrid Multi-carrier PWM technique based on carrier reconstruction and the correctness of theoretical analysis, an experimental platform of CHB Seven-level inverter is built as shown in Fig. 15. The experimental platform is controlled by FPGA+DSP, TX-KP101 is used as the drive, and the switch tube is IGBT IXGH12N60BD1. The experimental parameters are: DC side voltage E is 100V, reconstructed carrier frequency $f_c^{'} = 3$KHz, fundamental frequency $f_s = 50$Hz, filter inductance L = 4mH, Light load resistance $R_1 = 20\Omega$, Heavy load resistance $R_2 = 10\Omega$.

Fig. 16 shows the experimental waveforms of u_{Hi}, u_{AN} with Hybrid Multi-carrier PWM technique. It can be seen from the figure that the output voltage of each cell is a three-level high-frequency PWM waveform with a slight phase displacement between them, which is caused by the phase-shifted reconstructed carriers. u_{AN} is a seven-level high frequency PWM voltage waveform.

Fig. 17(a) and (b) shows the experimental waveforms of u_{Hi}, u_{AN}, and i_o with Hybrid Multi-carrier PWM technique at $m_a = 0.3$ and $m_a = 0.9$ respectively when the load resistance is suddenly changed (loading 100% and deloading 100%). As can be seen from the figure, when $m_a = 0.3$, u_{AN} is a three-level PWM waveform, because when $0 < m_a < 1/3$, it can be seen in Fig. 4(b) that the inverter can only output three levels $\pm E$, 0. The output current i_o waveform is quite different from the standard sinusoidal waveform.

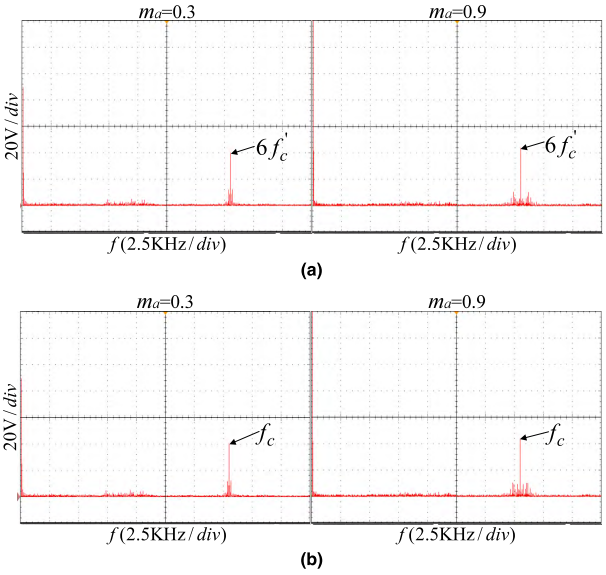

FIGURE 18. Harmonic Spectrum of u_{AN}. (a) with Hybrid Multi-carrier PWM technique. (b) with IPD-PWM technique.

The previous simulation has shown that when $m_a = 0.3$, the harmonic content of u_{AN} reaches 64.39%, which leads to the poor quality of the output current waveform. However, when $m_a = 0.9$, u_{AN} is a Seven-level PWM waveform, and its harmonic content is as low as 22.43%. The quality of the output current waveform is obviously improved. Under the two modulation indexs, the amplitude of i_o is

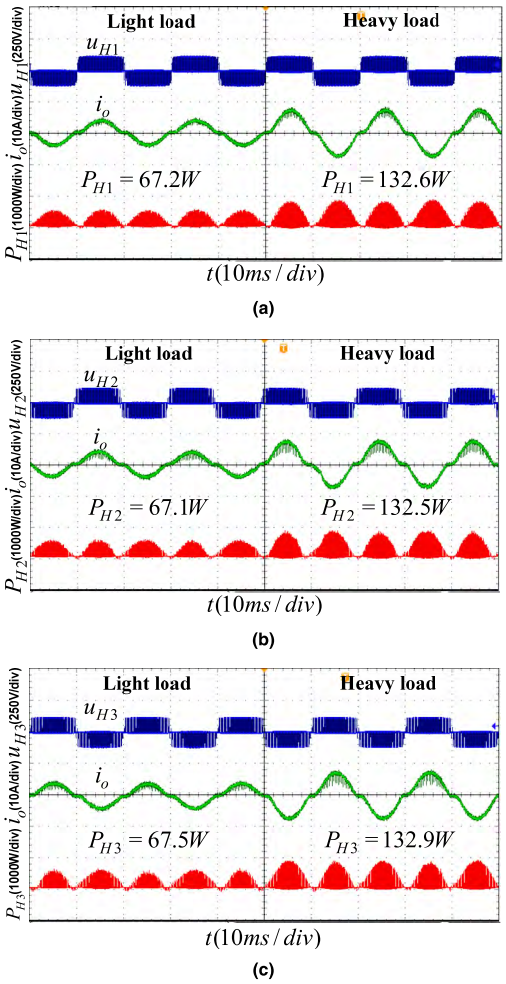

FIGURE 19. Experimental waveforms of each H-bridge cell at $m_a = 0.3$. (a) H1-bridge cell. (b) H2-bridge cell. (c) H3-bridge cell.

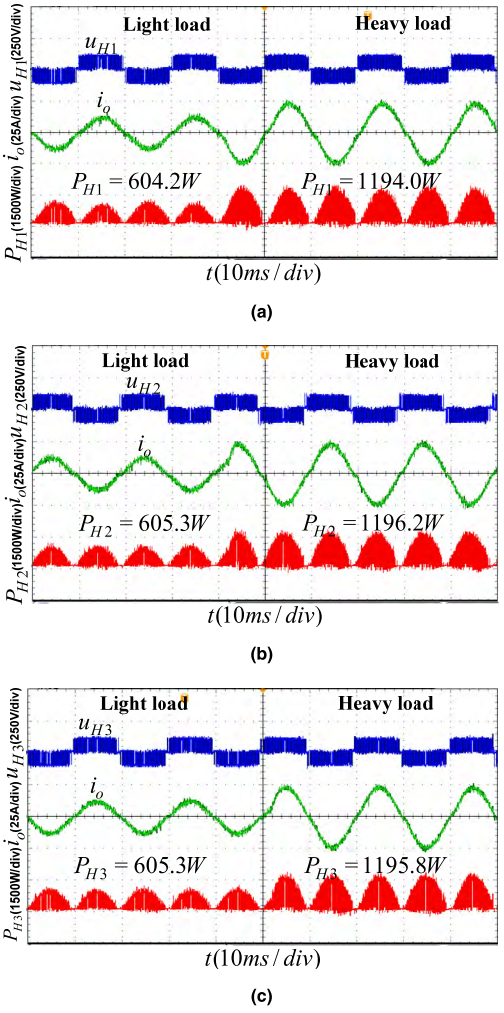

FIGURE 20. Experimental waveforms of each H-bridge cell at $m_a = 0.9$. (a) H1-bridge cell. (b) H2-bridge cell. (c) H3-bridge cell.

changed significantly when the load is suddenly changed, and the waveform of u_{AN} does not change. This indicates that the load has no effect on the waveform quality of u_{AN}. And the adjustment time of the transition process is very short.

Fig. 18(a) is the harmonic spectrum of u_{AN} under Hybrid Multi-carrier PWM technique at $m_a = 0.3$ and $m_a = 0.9$ respectively.

Fig. 18(b) is the harmonic spectrum of u_{AN} under IPD-PWM technique at $m_a = 0.3$ and $m_a = 0.9$ respectively.

The carrier frequency of IPD-PWM technique is set to 18KHZ. By comparison, whether at low or high modulation index, the harmonic spectrum of u_{AN} is almost identical under the two techniques. Under Hybrid Multi-carrier PWM technique, the high-frequency harmonic components mainly concentrate on the $6f_c^{'}$ and its side-band harmonics; Under IPD-PWM technique, the high-frequency harmonic components mainly concentrate on the f_c and its side-band harmonics. The spectrum of the two techniques does not contain low-frequency harmonics.

Fig. 19 and Fig. 20 are experimental waveforms of u_{Hi}, i_o, and p_{Hi} at $m_a = 0.3$ and $m_a = 0.9$ respectively When the load resistance is suddenly changed (loading 100%).

Obviously, whether at low or high modulation index, light load or heavy load, the output power p_{Hi} of each H-bridge cell is approximately equal. Therefore, Hybrid Multi-carrier PWM proposed in the paper can achieve output power balance naturally between cascaded H-bridge cells as in the case of CPS-PWM technique. At the moment of loading, the output current and output power of the inverter increase significantly, and the output voltage waveform of each cell does not change, so the load change has no effect on the output voltage and power balance control.

VI. CONCLUSIONS

Based on the analysis of the modulation principle of CPS-PWM and IPD-PWM techniques, this paper proposes a Hybrid Multi-carrier PWM modulation technique based on carrier reconstruction, which is applied to CHB seven-level

inverter, Through theoretical, simulation and experimental analysis, the results show that:

(1) The proposed Hybrid Multi-carrier PWM technique utilizes the redundant switching function states of the inverter to cyclically adjust the arrangement of the carrier in the vertical direction, so that the fundamental components of the output voltage of each cascaded H-bridge cell are equal. Therefore, the output power balance between cascaded H-bridge cells can be effectively realized, and the time required for power balance is one reconstructed carrier period.

(2) Under IPD-PWM and the proposed Hybrid Multi-carrier PWM technique, the fundamental component and harmonic spectrum of the inverter output voltage are exactly the same, that is, Hybrid Multi-carrier PWM technique proposed in this paper has the optimal harmonic characteristics of the output line voltage.

REFERENCES

[1] V. Jammala, S. Yellasiri, and A. K. Panda, "Development of a new hybrid multilevel inverter using modified carrier SPWM switching strategy," *IEEE Trans. Power Electron.*, vol. 33, no. 10, pp. 8192–8197, Oct. 2018.

[2] S. K. Sahoo and T. Bhattacharya, "Phase-shifted carrier-based synchronized sinusoidal PWM techniques for a cascaded H-bridge multilevel inverter," *IEEE Trans. Power Electron.*, vol. 33, no. 1, pp. 513–524, Jan. 2018.

[3] C. Oates, "Modular multilevel converter design for VSC HVDC applications," *IEEE J. Emerg. Sel. Topics Power Electron.*, vol. 3, no. 2, pp. 505–515, Jun. 2015.

[4] A. Ghias, P. Jose, and V. G. Agelidis, "A novel control method for transformerless H-bridge cascaded STATCOM with star configuration," *IEEE Trans. Power Electron.*, vol. 30, no. 3, pp. 1189–1202, Mar. 2015.

[5] M. Ye, L. Kang, Y. Xiao, P. Song, and S. Li, "Modified hybrid modulation strategy with power balance control for H-bridge hybrid cascaded seven-level inverter," *IET Power Electron.*, vol. 11, no. 6, pp. 1046–1054, Mar. 2018.

[6] M. Perez, S. Kouro, J. Rodriguez, and B. Wu, "Modified staircase modulation with low input current distortion for multicell converters," in *Proc. IEEE Electron. Spec. Conf. (PESC)*, Jun. 2008, pp. 1989–1994.

[7] M. S. A. Dahidah and V. G. Agelidis, "Selective harmonic elimination PWM control for cascaded multilevel voltage source converters: A generalized formula," *IEEE Trans. Power Electron.*, vol. 23, no. 4, pp. 1620–1630, Jul. 2008.

[8] P. W. Hammond, "A new approach to enhance power quality for medium voltage AC drives," *IEEE Trans. Ind Appl.*, vol. 33, no. 1, pp. 202–208, Jan. 1997.

[9] A. Razi, A. S. A. Wahab, and S. A. A. Shukor, "Improved wave shape-pattern performance using phase opposite disposition (POD) method for cascaded multilevel inverter," in *Proc. IEEE 2nd Annu. Southern Electron. Conf. (SPEC)*, Auckland, New Zealand, Dec. 2016, pp. 1–6.

[10] W. Yao, H. Hu, and Z. Lu, "Comparisons of space-vector modulation and carrier-based modulation of multilevel inverter," *IEEE Trans. Power Electron.*, vol. 23, no. 1, pp. 45–51, Jan. 2008.

[11] B. P. McGrath and D. G. Holmes, "Multicarrier PWM strategies for multilevel inverters," *IEEE Trans. Ind. Electron.*, vol. 49, no. 4, pp. 858–867, Aug. 2002.

[12] Y. Li, Y. Wang, and B. Q. Li, "Generalized theory of phase-shifted carrier PWM for cascaded H-bridge converters and modular multilevel converters," *IEEE J. Emerg. Sel. Topics Power Electron.*, vol. 4, no. 2, pp. 589–605, Jun. 2016.

[13] G. Carrara, S. Gardella, M. Marchesoni, R. Salutari, and G. Sciutto, "A new multilevel PWM method: A theoretical analysis," *IEEE Trans. Power Electron.*, vol. 7, no. 3, pp. 497–505, Jul. 1992.

[14] J. Liu, Y. Sun, Y. Li, and C. Fu, "Theoretical harmonic analysis of cascaded H-bridge inverter under hybrid pulse width multilevel modulation," *IET Power Electron.*, vol. 9, no. 14, pp. 2714–2722, Aug. 2016.

[15] P. Omer, J. Kumar, and B. S. Surjan, "Comparison of multicarrier PWM techniques for cascaded H-bridge inverter," in *Proc. IEEE Students' Conf. Elect., Electron. Comput. Sci.*, Mar. 2014, pp. 1–6.

[16] I. Sarkar and B. G. Fernandes, "Modified hybrid multi-carrier PWM technique for cascaded H-bridge multilevel inverter," in *Proc. IEEE 40th Annu. Conf. Ind. Electron. Soc.*, Oct. 2014, pp. 4318–4324.

[17] V. G. Agelidis and M. Calais, "Application specific harmonic performance evaluation of multicarrier PWM techniques," in *Proc. IEEE Rec. 29th Annu. Power Electron. Spec. Conf. (PESC)*, vol. 1, May 1998, pp. 172–178.

[18] L. M. Tolbert, F. Z. Peng, and T. G. Habetler, "Multilevel PWM methods at low modulation indices," *IEEE Trans. Power Electron.*, vol. 15, no. 4, pp. 719–725, Jul. 2000.

[19] D. Sreenivasarao, P. Agarwal, and B. Das, "Performance evaluation of carrier rotation strategy in level-shifted pulse-width modulation technique," *IET Power Electron.*, vol. 7, no. 3, pp. 667–680, Oct. 2013.

MANYUAN YE received the B.Eng. degree in industrial automation from the Anhui University of Science and Technology, Huainan, China, in 2001, and the M.Sc. degree in traffic control and information engineering from the East China Jiaotong University (ECJTU), Nanchang, China, in 2004, where he is currently pursuing the Ph.D. degree.

He is currently an Associate Professor with the School of Electrical and Automation Engineering, ECJTU. His research interests include power electronics and electric drives, modular multilevel converter, pulse width modulation, and selective harmonic elimination techniques.

LE CHEN received the B.Eng. degree in electrical engineering from the Shaanxi University of Science and Technology, Xi'an, China, in 2016. He is currently pursuing the M.Sc. degree with East China Jiaotong University, Nanchang, China. His research interests include power electronics and cascaded multilevel converter.

LIXUAN KANG received the B.Eng. degree in electrical engineering from the Nanchan Hangkong University, Nanchang, China, in 2016. He is currently pursuing the M.Sc. degree with East China Jiaotong University, Nanchang. His research interests include power electronics and cascaded multilevel converter.

SONG LI received the M.Sc. degree in traffic control and information engineering from the East China Jiaotong University (ECJTU), Nanchang, China, in 2005, where she is currently an Associate Professor with the School of Electrical and Automation Engineering. Her research interest includes power electronics.

JUNFEI ZHANG received the B.Eng. degree in electrical engineering from the Jiangxi University of Science and Technology, Nanchang, China, in 2016. He is currently pursuing the M.Sc. degree with the East China Jiaotong University, Nanchang. His research interests include power electronics and cascaded multilevel converter.

HAN WU received the B.Eng. degree in electrical engineering from Qufu Normal University, Rizhao, China, in 2017. He is currently pursuing the M.Sc. degree with the East China Jiaotong University, Nanchang, China. His research interests include power electronics and cascaded multilevel converter.